

RESEARCH-ARTICLE



Nonlinear vibration study of fiber-reinforced composite thin plate with strain-dependent property based on strain energy density function method

Hui Li , Pengcheng Xue, Tinan Zhang, and Bangchun Wen

School of Mechanical Engineering and Automation, Key Laboratory of Vibration and Control of Aero-Propulsion Systems, Ministry of Education of China, Northeastern University, Shenyang, PR China

ABSTRACT

The strain energy density function method is proposed to study the nonlinear vibration behavior of the fiber-reinforced composite thin plate with strain dependence. First, the material nonlinearity of the fiber-reinforced composite is extended to the vibration field. On the basis of Jones-Nelson nonlinear model, a theoretical model with the consideration of the strain-dependent nonlinearity is established to illustrate the theoretical principle of the strain energy density function method. In the model, the nonlinear elastic moduli in different fiber directions are expressed as a function of the strain energy density. The nonlinear natural frequencies are solved by Ritz method in conjunction with the classical laminated plate theory and Hamilton's principle, and the nonlinear vibration responses are calculated by Newton-Raphson iteration method. Moreover, a TC300 carbon/epoxy composite plate is taken as a research object. In order to determine the corresponding parameters in the theoretical model, the composite beam specimens are cut off to conduct the stress-strain measurement. The nonlinear natural frequencies and vibration responses of the composite plate under different excitation levels are obtained. The comparisons between the theoretical calculation and experimental test show that the maximum calculation error of the first six natural frequencies with considering the strain-dependent nonlinearity is less than 4.3%, and the maximum calculation error of the resonant responses is less than 12.0% for the third mode and the sixth mode, thus the practicability and reliability of the proposed method have been verified.

ARTICLE HISTORY

Received 13 March 2018
Revised 13 May 2018
Accepted 28 June 2018

KEYWORDS



Fiber-reinforced composite thin plate; nonlinear vibration; strain dependent property; strain energy density function method; iterative calculation

1. Introduction

The fiber-reinforced composite has excellent mechanical properties, good thermal stability, and capability with light weight; thus it has been widely used in the aeronautics, astronautics, automotive, naval vessel, and weapon industries [1–2]. Currently, there are a large number of composite thin plate structures, such as the solar panels, aircraft engine fan blades, large wind turbine blades, etc. The vibration problems of such composite blades and plates have been increasingly severe in the harsh environment [3]. Besides, it has been found that these fiber-reinforced composite plate structures show the nonlinear stiffness properties, which is obviously different from the traditional isotropic plate structures. For example, their natural frequencies can change with different external excitation levels or strain levels, which show some nonlinear stiffness characteristics. These nonlinear characteristics have brought great difficulties and challenges to the traditional analysis methods based on linear equivalent principle mainly. Therefore, it is of great scientific significance to study the nonlinear vibration characteristics of such composite plate structures and the corresponding analysis techniques [4].

In recent years, there have been increasing concerns about the nonlinear modeling and analysis methods of static

and dynamic characteristics of the plate-like fiber-reinforced composite structures. Stecenko and Stevanovi [5] studied the strain dependence behavior of the tensile and compressive elastic moduli in carbon fiber/epoxy resin unidirectional and multidirectional composite plates. Rao and Pillai [6] analyzed the large-amplitude vibrations of a simply supported composite plate with immovable edges. The Kirchhoff's hypothesis and the strain-displacement relations of von Kármán type were used in the formulation of the in-plane deformation. Singh et al. [7] presented a direct numerical integration method of the frequency/time period expression to study the nonlinear vibration behavior of the fiber-reinforced plates and also obtained the governing equations of motion based on the Von Kármán relationships. Ribeiro and Petyt [8] studied the geometrically nonlinear vibration of a thin laminated composite plate under fully clamped boundary condition by the hierarchical finite element and the harmonic balance method. Chen et al. [9] presented the semi-analytical finite strip method to analyze the geometrically nonlinear response of the rectangular composite laminated plates under the simply supported boundary condition. Lee and Ng [10] proposed a time-domain modal formulation using the finite element method for the large-amplitude vibrations of the composite thin plates. Harras et al. [11]

CONTACT Hui Li  lh200300206@163.com  School of Mechanical Engineering and Automation, Northeastern University, Key Laboratory of Vibration and Control of Aero-Propulsion Systems, Ministry of Education of China, Northeastern University, Liaoning, Shenyang 110819, PR China

© 2018 Taylor & Francis Group, LLC

established a theoretical model of the nonlinear vibration of the thin composite plate based on the von Kármán strain-displacement relations. Toyama and Takatsubo [12] proposed a new method to measure the tensile strain using Lamb waves, and the nonlinear elastic behavior of the unidirectional and cross-ply composite plate was also investigated. Onkar and Yadav [13] conducted the nonlinear random vibration analysis on the composite laminated plates based on the Kirchhoff-Love plate theory and Von Kármán nonlinear strain-displacement relationships. Tabiei et al. [14] proposed the nonlinear strain-rate-dependent composite material model, which can be used for simulating the behavior of composite structures under the various loads such as impact and tensile loading. Zhu et al. [15] investigated the effects of strain rate dependency and inelasticity on the transient responses of the composite thin plates. Singha and Daripa [16] studied the large amplitude vibration behavior of the composite thin plates based on the von Kármán's assumptions, and the time history for the nonlinear vibration was obtained by Newmark's time integration technique. Zafer and Zahit [17] studied the nonlinear dynamic response of a laminated composite plate under the simply supported boundary condition subject to blast load, and the geometric nonlinearity effects were also taken into account with the von Kármán large deflection theory. Singha and Daripa [18] used the shear deformable finite element method to analyze the large amplitude vibration characteristics of a composite plate under transverse harmonic pressure or periodic in-plane load. Arani et al. [19] used an analytical approach as well as the finite element method to study the buckling of laminated composite plates reinforced by single-walled carbon nanotubes. Arani and Jafari [20] studied the nonlocal nonlinear vibration analysis of embedded laminated microplates resting on an elastic matrix as an orthotropic Pasternak medium. The governing equations were derived based on the orthotropic Mindlin plate theory along with the von Kármán geometric nonlinearity and Hamilton's principle. Arani et al. [21] also studied modeling and vibration control of axially moving laminated carbon nanotubes/fiber/polymer composite (CNTFPC) plate under initial tension. Setoodeh and Shojaee [22] used the differential quadrature method in conjunction with the tainted weighing coefficients to solve geometrically nonlinear vibration of functionally graded carbon nanotube-reinforced composite plates. Jiang et al. [23] studied nonlinear vibration characteristics of composite laminated trapezoidal plates considering the geometric nonlinearity based on the von Kármán strain-displacement relations. Chai et al. [24] studied the nonlinear vibrations of composite laminated plates with time-dependent base excitation and boundary conditions. Jones and Nelson [25] and Jones and Morgan [26] proposed a new material model for the deformation behavior of the fiber-reinforced composite under the static loading. They believed that the nonlinear stress-strain behavior was mainly due to the nonlinear matrix material which greatly affected the transverse modulus and the shear modulus, so they expressed the material parameters as a function of strain energy density and verified the effectiveness by comparing with the experiments and the other literatures.

Although the aforementioned researches have deeply investigated the nonlinear vibration characteristics of the fiber-reinforced composite plates, most of them only studied the geometric nonlinearity of the composite plates based on the Von Kármán strain-displacement relationships. Besides, a few scholars [25,26] employed the nonlinear material theory to clarify the nonlinear stress-strain relations of the composite structures, but their main concern is the static nonlinear behavior, and the nonlinearity of the fiber-reinforced composite has not been introduced in the nonlinear vibration modeling of the structures. Therefore, it is still necessary to put great efforts to study the nonlinear vibration problems of such composite plate structures, especially providing an appropriate mathematical model and analytical method to describe the nonlinear vibration phenomenon with strain dependence.

In this article, the material nonlinearity of the fiber-reinforced composite is extended to the vibration field. On the basis of Jones-Nelson nonlinear model, the strain energy density function method is proposed to investigate the nonlinear vibration behavior of the fiber-reinforced composite thin plate with strain dependence. In Section 2, the elastic modulus of the fiber composite is expressed as a function of the strain energy density, and the theoretical model is established by Ritz method, so that its nonlinear natural frequencies and vibration responses can be iteratively calculated. Then, after the theoretical principle is illustrated, we go on to propose the specific analysis procedure of the nonlinear natural frequencies and vibration responses in Section 3. Finally, in Section 4, a TC300 carbon/epoxy composite plate is taken as a research object, and the nonlinear natural frequencies and vibration responses under different excitation levels are obtained in the experiment. By comparing the experimental results with the calculated linear and nonlinear frequency and response results with and without considering the strain-dependent nonlinearity, the practicability, and reliability of the proposed method have been verified.

2. Theoretical principle of the strain energy density function method

In this section, the strain energy density function method is proposed to study the nonlinear vibration of the fiber-reinforced composite thin plate with strain-dependent property, and the corresponding theoretical principle is explained in details.

2.1. Theoretical model

The fiber-reinforced composite thin plate is made of fiber and matrix material with n layers, as seen in Figure 1. First, set up the coordinate system xoy at the middle surface, and the length, width, and thickness of the composite plate are assumed to be a , b , and h , while the fiber direction within a layer is defined as θ from the x -axes of coordinate system xoy . In this model, each layer is located at h_{k-1} and h_k along the z -axes with equal thickness. "1" represents the direction parallel to the fiber, "2" represents the direction

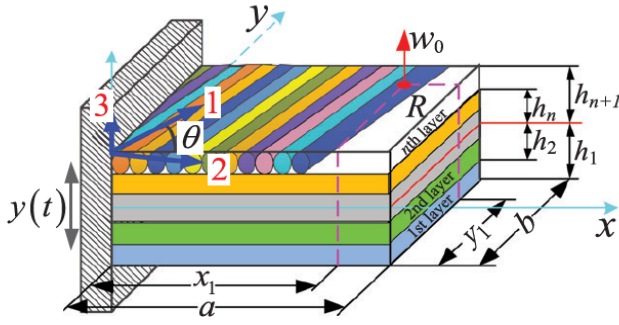


Figure 1. A theoretical model of fiber-reinforced composite thin plate. (a) analysis procedure of the nonlinear natural frequency and (b) analysis procedure of the nonlinear vibration response.

perpendicular to the fiber, and “3” represents the direction perpendicular to the 1–2 surface. Besides, assuming that the composite plate is under cantilever boundary condition, $R(x_1, y_1)$ is vibration response point and the base excitation load with the expression $y(t) = Ye^{i\omega t}$ is applied on its constraint side, where Y is the base excitation amplitude, ω is the excitation angular frequency, and t is the time. The elastic moduli of the layer parallel and perpendicular to the fiber are E_1 and E_2 , the shear modulus in the 1–2 surface is G_{12} , the related Poisson’s ratios which are induced by the stress in “1” and “2” direction are ν_{12} and ν_{21} , and the density is ρ .

According to the Jones-Nelson nonlinear theory [25,26], the modulus in any point of the stress-strain curve of the fiber composite can be expressed as the function of strain energy density, whose expression can be defined as

$$Y_{\text{non}i} = Y_{0i} \left[1 - A_i \left(\frac{U^*}{U_{0i}^*} \right)^{B_i} \right] \quad (i = 1, 2, 12) \quad (1)$$

where $Y_{\text{non}i}$ is the nonlinear elastic moduli in different fiber directions (such as 1, 2, and 1–2 directions), Y_{0i} is the corresponding initial values, and A_i, B_i are the initial curvature and the corresponding variation of the stress-strain curves of fiber-reinforced composite in the longitudinal, transverse, and shear directions. By referring the literature [25,26], A_i, B_i are dimensionless and can be determined by fitting the expression of the measured longitudinal, transverse, and shear stress-strain curves of the fiber composite with the cubic polynomial fitting algorithm. Besides, the constant U_{0i}^* is included in Eq. (1) to help make strain energy density of U^* dimensionless. The numerical value of U_{0i}^* is arbitrary and should be selected before the values of A_i and B_i are determined.

According to the definition of the strain energy density, U^* can be expressed as follows

$$U^* = \frac{\frac{1}{2} \int_0^a \int_0^b \int_0^h \sigma_x \varepsilon_x + \sigma_y \varepsilon_y + \sigma_{xy} \gamma_{xy} dx dy dz}{abh} \quad (2)$$

Then, the nonlinear material parameter of the fiber-reinforced plate can be expressed as

$$E_{\text{non}1} = E_1 \left[1 - A_1 \left(\frac{U^*}{U_{01}^*} \right)^{B_1} \right] \quad (3)$$

$$E_{\text{non}2} = E_2 \left[1 - A_2 \left(\frac{U^*}{U_{02}^*} \right)^{B_2} \right] \quad (4)$$

$$G_{\text{non}12} = G_{12} \left[1 - A_{12} \left(\frac{U^*}{U_{012}^*} \right)^{B_{12}} \right] \quad (5)$$

Because the concerned fiber-reinforced composite plate is symmetrical between the middle surface, its inner and outer displacements are decoupled. Then, according to the classical laminate theory [27], the displacement field can be expressed as

$$\begin{aligned} u(x, y, z, t) &= u_0(x, y, t) - z \frac{\partial w_0(x, y, t)}{\partial x} \\ v(x, y, z, t) &= v_0(x, y, t) - z \frac{\partial w_0(x, y, t)}{\partial y} \\ w(x, y, z, t) &= w_0(x, y, t) \end{aligned} \quad (6)$$

where u, v, w represent the displacements of any point of the composite plate, and u_0, v_0, w_0 are the displacements in the midplane. Besides, h is the thickness and t is the time.

Based on the assumed displacement field of the classical laminate theory, the normal strain ε_z , shear strain γ_{yz} and γ_{xz} of the composite plate are equal to zero, i.e., $\varepsilon_z = \gamma_{yz} = \gamma_{xz} = 0$. Then, considering the relationship between strain and displacement, the strain of any point in the plate can be obtained

$$\begin{aligned} \varepsilon_x &= \frac{\partial u}{\partial x} = -z \frac{\partial^2 w_0}{\partial x^2} \\ \varepsilon_y &= \frac{\partial v}{\partial y} = -z \frac{\partial^2 w_0}{\partial y^2} \\ \gamma_{xy} &= \frac{\partial u}{\partial y} + \frac{\partial v}{\partial x} = -2z \frac{\partial^2 w_0}{\partial x \partial y} \end{aligned} \quad (7)$$

The bending curvatures κ_x, κ_y and torsion curvature κ_{xy} of the composite plate in the middle surface can be expressed as

$$\kappa_x = -\frac{\partial^2 w_0}{\partial x^2}, \kappa_y = -\frac{\partial^2 w_0}{\partial y^2}, \kappa_{xy} = -2 \frac{\partial^2 w_0}{\partial x \partial y} \quad (8)$$

The strain of any point in the composite plate can be simplified as

$$\varepsilon_x = z\kappa_x, \varepsilon_y = z\kappa_y, \gamma_{xy} = z\kappa_{xy}$$

For the orthotropic material, the stress-strain relationship in the fiber coordinates can be defined as

$$\begin{Bmatrix} \sigma_1 \\ \sigma_2 \\ \sigma_{12} \end{Bmatrix} = \begin{bmatrix} Q_{11} & Q_{12} & 0 \\ Q_{21} & Q_{22} & 0 \\ 0 & 0 & Q_{66} \end{bmatrix} \begin{Bmatrix} \varepsilon_1 \\ \varepsilon_2 \\ \gamma_{12} \end{Bmatrix} \quad (9)$$

where

$$\begin{aligned} Q_{11} &= \frac{E_{\text{non}1}}{1 - \nu_{12}\nu_{21}}, \quad Q_{12} = \frac{\nu_{12}E_{\text{non}2}}{1 - \nu_{12}\nu_{21}} \\ Q_{22} &= \frac{E_{\text{non}2}}{1 - \nu_{12}\nu_{21}}, \quad Q_{66} = G_{\text{non}12}, \quad \nu_{21} = \nu_{12} \frac{E_{\text{non}2}}{E_{\text{non}1}} \end{aligned} \quad (10)$$

When an angle of θ exists between the fiber coordinates and global coordinates, the stress-strain relationship of the k th layer of the composite plates in the global coordinates can

be calculated by using the stress-strain transformation equation [28], which can be expressed in the following form

$$\begin{aligned} \begin{Bmatrix} \sigma_x \\ \sigma_y \\ \sigma_{xy} \end{Bmatrix}^{(k)} &= \begin{bmatrix} \bar{Q}_{11} & \bar{Q}_{12} & \bar{Q}_{16} \\ \bar{Q}_{12} & \bar{Q}_{22} & \bar{Q}_{26} \\ \bar{Q}_{16} & \bar{Q}_{26} & \bar{Q}_{66} \end{bmatrix}^{(k)} \begin{Bmatrix} \varepsilon_x \\ \varepsilon_y \\ \gamma_{xy} \end{Bmatrix} \\ &= \begin{bmatrix} \bar{Q}_{11} & \bar{Q}_{12} & \bar{Q}_{16} \\ \bar{Q}_{12} & \bar{Q}_{22} & \bar{Q}_{26} \\ \bar{Q}_{16} & \bar{Q}_{26} & \bar{Q}_{66} \end{bmatrix}^{(k)} \begin{Bmatrix} z\kappa_x \\ z\kappa_y \\ z\kappa_{xy} \end{Bmatrix} \end{aligned} \quad (11)$$

where

$$\begin{aligned} \bar{Q}_{11} &= Q_{11} \cos^4 \theta_k + 2(Q_{12} + 2Q_{66}) \sin^2 \theta_k \cos^2 \theta_k + Q_{22} \sin^4 \theta_k \\ \bar{Q}_{12} &= (Q_{11} + Q_{22} - 4Q_{66}) \sin^2 \theta_k \cos^2 \theta_k \\ &\quad + Q_{12} (\sin^4 \theta_k + \cos^4 \theta_k) \\ \bar{Q}_{22} &= Q_{11} \sin^4 \theta_k + 2(Q_{12} + 2Q_{66}) \sin^2 \theta_k \cos^2 \theta_k + Q_{22} \cos^4 \theta_k \\ \bar{Q}_{16} &= (Q_{11} - Q_{12} - 2Q_{66}) \sin \theta_k \cos^3 \theta_k \\ &\quad + (Q_{12} - Q_{22} + 2Q_{66}) \sin^3 \theta_k \cos \theta_k \\ \bar{Q}_{26} &= (Q_{11} - Q_{12} - 2Q_{66}) \sin^3 \theta_k \cos \theta_k \\ &\quad + (Q_{12} - Q_{22} + 2Q_{66}) \sin \theta_k \cos^3 \theta_k \\ \bar{Q}_{66} &= (Q_{11} + Q_{22} - 2Q_{12} - 2Q_{66}) \sin^2 \theta_k \cos^2 \theta_k \\ &\quad + Q_{66} (\sin^4 \theta_k + \cos^4 \theta_k) \end{aligned} \quad (12)$$

where k represents the k th layer of the composite plate, θ_k represents the angle between the fiber direction in fiber coordinates and the x direction in the global coordinates.

The bending and twisting moment resultants in the composite plate can be expressed as

$$\begin{aligned} \begin{bmatrix} M_x \\ M_y \\ M_{xy} \end{bmatrix} &= \sum_{k=1}^n \int_{z_{k-1}}^{z_k} \begin{bmatrix} \sigma_x \\ \sigma_y \\ \sigma_{xy} \end{bmatrix}^{(k)} z dz \\ &= \sum_{k=1}^n \int_{z_{k-1}}^{z_k} \begin{bmatrix} \bar{Q}_{11} & \bar{Q}_{12} & \bar{Q}_{16} \\ \bar{Q}_{12} & \bar{Q}_{22} & \bar{Q}_{26} \\ \bar{Q}_{16} & \bar{Q}_{26} & \bar{Q}_{66} \end{bmatrix}^{(k)} \begin{Bmatrix} z\kappa_x \\ z\kappa_y \\ z\kappa_{xy} \end{Bmatrix} z dz \\ &= \begin{bmatrix} D_{11} & D_{12} & D_{16} \\ D_{12} & D_{22} & D_{26} \\ D_{16} & D_{26} & D_{66} \end{bmatrix} \begin{Bmatrix} \kappa_x \\ \kappa_y \\ \kappa_{xy} \end{Bmatrix} \end{aligned} \quad (13)$$

where

$$D_{ij} = \frac{1}{3} \sum_{k=1}^n \left(\bar{Q}_{ij} \right)^{(k)} (z_k^3 - z_{k-1}^3), \quad i, j = 1, 2, 6$$

Assuming that the base excitation applied on the composite plate can be simplified as the external load of the uniform inertia force $f(t)$, which has the following expression

$$f(t) = -\rho h \frac{d^2 y(t)}{dt^2} = \rho h Y \omega^2 e^{i\omega t} \quad (14)$$

The bending strain energy U stored in the composite plate can be expressed as

$$U = \frac{1}{2} \iint_R [M_x \kappa_x + M_y \kappa_y + M_{xy} \kappa_{xy}] dx dy \quad (15)$$

The kinetic energy T of the composite plate can be expressed as

$$T = \frac{\rho h}{2} \iint_R \left(\frac{\partial w_0}{\partial t} \right)^2 dx dy \quad (16)$$

The external work W_f done by the uniform inertia force is

$$W_f = \iint_R f(t) w_0 dx dy \quad (17)$$

The damping work W_c done by the equivalent viscous damping is

$$W_c = \iint_R c \left(\frac{\partial w_0}{\partial t} \right) w_0 dx dy \quad (18)$$

where c is the viscous damping coefficient.

2.2. Nonlinear vibration solution

Assuming that the displacement of any vibration response point $R(x_1, y_1)$ in the composite plate is w_0 , as seen in Figure 1, which can be expressed as

$$w_0 = e^{i\omega t} W(\xi, \eta) \quad (19)$$

where $W(\xi, \eta)$ represents the modal shape function which can be defined as

$$W(\xi, \eta) = \sum_{i=1}^M \sum_{j=1}^N q_{ij} P_i(\xi) P_j(\eta) \quad (20)$$

where q_{ij} are the eigenvectors which need to be solved, and $P_i(\xi)$ ($i = 1, \dots, M$) and $P_j(\eta)$ ($j = 1, \dots, N$) are the orthogonal polynomials.

Then, the orthogonal polynomials can be obtained by implementing the orthogonalization operation on polynomial function, which should satisfy the boundary condition of the composite plate, and these polynomials have the following expressions

$$\begin{aligned} P_1(\xi) &= \chi(\xi), \quad P_1(\eta) = \kappa(\eta) \\ P_2(\phi) &= (\phi - H_2) P_1(\phi) \\ P_i(\phi) &= (\phi - H_i) P_{i-1}(\phi) - V_i P_{i-2}(\phi) \\ \phi &= \xi, \eta, \quad i > 2 \end{aligned} \quad (21)$$

where H_i and V_i are the coefficient functions and their expressions can be written as

$$\begin{aligned} H_i &= \frac{\int_0^1 W(\phi) [P_{i-1}(\phi)]^2 \phi d\phi}{\int_0^1 W(\phi) [P_{i-1}(\phi)]^2 d\phi} \\ V_i &= \frac{\int_0^1 W(\phi) P_{i-1}(\phi) P_{i-2}(\phi) \phi d\phi}{\int_0^1 W(\phi) [P_{i-2}(\phi)]^2 d\phi}, \quad \phi = \xi, \eta \end{aligned} \quad (22)$$

where $W(\phi)$ is the weighting function and $W(\phi) = 1$ is usually used. Besides, $\chi(\xi)$ and $\kappa(\eta)$ are the polynomial functions which can satisfy different boundary conditions, such as the clamped, simply supported and free boundary. They can be expressed as

$$\begin{aligned} \chi(\xi) &= \xi^\alpha (1 - \xi)^\beta, \quad \kappa(\eta) = \eta^\gamma (1 - \eta)^\tau \\ \xi &= x/a, \quad \eta = y/b \end{aligned} \quad (23)$$

Because the studied composite plate is under the cantilever boundary condition, we can set $\alpha = 2, \beta = 0, \gamma = 0, \tau = 0$. Then, by substituting Eq. (19) into Eq. (15) to Eq. (18), the maximum bending strain energy U_{\max} stored in the plate, the maximum kinetic energy T_{\max} , the maximum external work $W_{f\max}$ done by the uniform inertia force and the maximum damping work $W_{c\max}$ done by the equivalent viscous damping can be obtained and expressed as

$$U_{\max} = \frac{1}{2} \iint_R \left[D_{11} \left(\frac{\partial^2 W}{\partial x^2} \right)^2 + 2D_{12} \frac{\partial^2 W}{\partial x^2} \frac{\partial^2 W}{\partial y^2} + D_{22} \left(\frac{\partial^2 W}{\partial y^2} \right)^2 + 4 \left(D_{16} \frac{\partial^2 W}{\partial x^2} + D_{26} \frac{\partial^2 W}{\partial y^2} \right) \frac{\partial^2 W}{\partial x \partial y} + 4D_{66} \left(\frac{\partial^2 W}{\partial x \partial y} \right)^2 \right] dx dy \quad (24)$$

$$T_{\max} = \frac{\rho h \omega^2}{2} \iint_R (W)^2 dx dy \quad (25)$$

$$W_{f\max} = \rho h Y \omega^2 \iint_R W dx dy \quad (26)$$

$$W_{c\max} = i\omega \iint_R c W^2 dx dy \quad (27)$$

Next, define the Lagrangian energy function L as

$$L = T_{\max} + W_{f\max} - U_{\max} - W_{c\max} \quad (28)$$

By minimizing the partial derivative of the Lagrangian energy function L with respect to q_{ij} in the following equation

$$\frac{\partial L}{\partial q_{ij}} = 0, i = 1, 2, \dots, M, \quad j = 1, 2, \dots, N \quad (29)$$

Because $M \times N$ equations in frequency domain are obtained, the vibration equation of the fiber-reinforced composite plate with consideration of the strain-dependent nonlinear effects can be written as the following expression (If the plate is under the condition without considering such nonlinearity, then, K_{non} will be replaced by linear stiffness matrix K in the equation)

$$(K_{\text{non}} + i\omega C - \omega^2 M) \mathbf{q} = \mathbf{F} \quad (30)$$

where K_{non} , C and M are the nonlinear stiffness matrix, damping matrix, and mass matrix, respectively, $\mathbf{q} = (q_{11}, q_{12}, \dots, q_{ij})^T$ is the response vector, and \mathbf{F} is the exciting force vector.

For the damping matrix C , we can turn it into the diagonal matrix after the following transformation, which can be realized by introducing the modal damping ratio ζ_i obtained in the real experiment.

$$\zeta_i = \frac{c_i}{2m\omega_i} \quad (31)$$

where ω_i is the i th natural frequency and m is the mass of the plate.

Ignoring the damping matrix and the exciting force vector in Eq. (30), the free vibration eigenvalue equation of the

plate with considering the strain-dependent nonlinearity is obtained, which can be written as

$$(K_{\text{non}} - \omega^2 M) \mathbf{q} = 0 \quad (32)$$

In order to make Eq. (32) have nonzero solution or non-trivial solution, the determinant of the coefficient matrix should be equal to zero

$$|K_{\text{non}} - \omega_i^2 M| = 0 \quad (33)$$

In order to solve the nonlinear natural frequencies of the composite plate, the iteration technique is employed to solve Eq. (33) when the initial iteration value $\omega_i^{(0)}$ is settled. Besides, according to the minimum difference principle of the two adjacent natural frequency results, the iteration termination condition can be set as

$$|\omega_i^{(j+1)} - \omega_i^{(j)}| \leq S_0 \quad (34)$$

where S_0 is the iteration accuracy factor, $\omega_i^{(j)}$ is the j th step of the natural frequency results, $\omega_i^{(j+1)}$ is the $j+1$ th step of the natural frequency results (superscript j or $j+1$ represents the different iteration steps).

Finally, by solving Eq. (33) with iteration technique, the i th nonlinear natural frequency ω_i of the composite plate can be determined, whose calculation procedure will be described in detail in Section 3.

After the iteration calculation work of the nonlinear natural frequencies of the composite plate is finished, Newton-Raphson iteration method is employed to calculate its nonlinear vibration response. The expression of residual vector \mathbf{r} can be obtained through transposition treatment as follow.

$$\mathbf{r} = (K_{\text{non}} + i\omega C - \omega^2 M) \mathbf{q} - \mathbf{F} \quad (35)$$

Because \mathbf{r} is a complex vector which includes the real part \mathbf{q}_R and the imaginary part \mathbf{q}_I of the response vector \mathbf{q} , it can be written in the form of $\mathbf{q}_R + i\mathbf{q}_I$. Then, the Jacobian matrix J related to \mathbf{r} can be expressed as

$$J = \begin{bmatrix} R(\partial \mathbf{r} / \partial \mathbf{q}_R) & R(\partial \mathbf{r} / \partial \mathbf{q}_I) \\ I(\partial \mathbf{r} / \partial \mathbf{q}_R) & I(\partial \mathbf{r} / \partial \mathbf{q}_I) \end{bmatrix} \quad (36)$$

$$\frac{\partial \mathbf{r}}{\partial \mathbf{q}_R} = K_{\text{non}} + i\omega C - \omega^2 M \quad (37)$$

$$\frac{\partial \mathbf{r}}{\partial \mathbf{q}_I} = i(K_{\text{non}} + i\omega C - \omega^2 M) \quad (38)$$

Meanwhile, by separating the real and imaginary part of the residual vector \mathbf{r} and the response vector \mathbf{q} , the separation vectors of $\bar{\mathbf{r}}$ and $\bar{\mathbf{q}}$ can be obtained and expressed as

$$\bar{\mathbf{r}} = \begin{Bmatrix} R(\mathbf{r}) \\ I(\mathbf{r}) \end{Bmatrix} \quad (39)$$

$$\bar{\mathbf{q}} = \begin{Bmatrix} R(\mathbf{q}) \\ I(\mathbf{q}) \end{Bmatrix} \quad (40)$$

By combining Eq. (36) with Eq. (40), the Newton-Raphson iteration formula of Eq. (36) can be

expressed as

$$\bar{\mathbf{r}}^{(j)} + \mathbf{J}^{(j)} \times \Delta \bar{\mathbf{q}}^{(j)} = 0 \quad (41a)$$

$$\bar{\mathbf{q}}^{(j+1)} = \bar{\mathbf{q}}^{(j)} + \Delta \bar{\mathbf{q}}^{(j)} \quad (41b)$$

$$\mathbf{q}^{(j+1)} = \mathbf{R}(\bar{\mathbf{q}}^{(j+1)}) + \mathbf{i} \times \mathbf{I}(\bar{\mathbf{q}}^{(j+1)}) \quad (41c)$$

where $\Delta \bar{\mathbf{q}}^{(j)}$ represents the response increment in the j th step.

Finally, by substituting the initial iteration value of the resonant response $\mathbf{q}^{(0)}$ (when $j=0$) into Eq. (41), the iteration termination condition can be determined when 2-norm of residual vector \mathbf{r} is less than the iteration accuracy factor S_0 (e.g., set $S_0 = 0.0001$), which has the following form

$$\|\mathbf{r}^{(j+1)}\|_2 = \sqrt{(|\mathbf{r}_1^{(j+1)}|^2 + |\mathbf{r}_2^{(j+1)}|^2 + |\mathbf{r}_3^{(j+1)}|^2 + \dots)} \leq S_0 \quad (42)$$

When the 2-norm of residual vector \mathbf{r} in Eq. (42) satisfies the iteration termination condition, by using Eq. (41) the response vector \mathbf{q} can be acquired. Further, by substituting \mathbf{q} into Eq. (19), the nonlinear vibration response of the composite plate under a certain exciting frequency can be solved.

3. Analysis procedure of nonlinear vibration characteristics of composite thin plate

In this section, the analysis procedure of the nonlinear natural frequencies and vibration responses of the fiber-reinforced composite thin plate is proposed, which can be realized based on the self-designed MATLAB program.

1. Calculate the mass matrix, damping matrix, stiffness matrix, and excitation force vector without considering the strain-dependent nonlinearity.

First, input the following parameters: (I) the geometrical parameters of the composite plate, such as the length, width and thickness; (II) the material parameters without considering the nonlinearity, such as the longitudinal modulus E_1 , transverse modulus E_2 , shear modulus G_{12} , Poisson's ratio ν_{12} and density ρ ; (III) the laying parameters, such as the number of ply-layer and the laying angle of each layer. Then, assume the expression of the transverse vibration displacement, so as to obtain vibration mode function $W(\xi, \eta)$ by Schmidt orthogonalization of the orthogonal polynomials. Next, substitute the displacement expression (19) into Eq. (15) to Eq. (17)), and eliminate the influence of the harmonic components to obtain the maximum strain energy U_{\max} , the maximum kinetic energy T_{\max} , and the maximum external force work $W_{f\max}$. Further, substitute Eq. (24) to Eq. (26) into Eq. (28) to solve the partial derivative results, and the mass matrix, stiffness matrix, and external excitation force vector can be obtained. Finally, introduce the modal damping ratio ζ_i acquired in the experiment into the theoretical model to calculate damping matrix \mathbf{C} .

2. Calculate the initial iteration values of the natural frequency and vibration response at a certain excitation frequency without considering the strain-dependent nonlinearity.

In this step, the initial iteration value of the natural frequency $\omega_i^{(0)}$ can be obtained by solving the free vibration eigenvalue Eq. (32). Besides, the initial iteration value of the resonant response $\mathbf{q}^{(0)}$ at a certain natural frequency $\omega_i^{(0)}$ can be obtained by substituting $\omega_i^{(0)}$ into the vibration response Eq. (30) in the frequency domain without considering the strain-dependent nonlinearity of the composite plate.

3. Calculate the iterative initial value of the strain energy density.

In this step, first substitute the initial iteration value of the resonant response $\mathbf{q}^{(0)}$ calculated in the second step into Eq. (19) to obtain the displacement response w_0 . under the resonant condition. Then, by substituting w_0 into Eq. (2), the iterative initial value of the strain energy density $U^{*(0)}$ can be obtained.

4. Calculate the nonlinear material parameters and the nonlinear stiffness matrix.

First, substitute the iterative initial value of the strain energy density $U^{*(0)}$ calculated in the third step into Eq. (3) to Eq. (5) so as to obtain the nonlinear material parameters, such as $E_{\text{non}1}$, $E_{\text{non}2}$, and $G_{\text{non}12}$. Then, employ the same calculation method used in the first step, the nonlinear stiffness matrix \mathbf{K}_{non} can be acquired.

5. Iteratively calculate the nonlinear natural frequencies with an appropriate iteration accuracy factor.

In this step, in order to iteratively calculate the i th nonlinear natural frequency ω_i , it is necessary to set an appropriate iteration accuracy factor S_0 . If the resulting $\omega_i^{(j-1)}$ do not meet the requirement of S_0 , it is needed to recalculate the resonant response $\mathbf{q}^{(j)}$ by using $\omega_i^{(j)}$ as the excitation frequency. By carefully comparing the calculation results, when S_0 is equal to 0.0001, it is accurate enough to determine $\omega_i^{(j)}$. Repeating the step (3) to the step (5), the nonlinear natural frequency results in the other modes can also be sequentially acquired.

6. Calculate the residual vector and Jacobian matrix.

First, substitute the mass matrix, damping matrix, stiffness matrix, and external excitation force vector obtained in the step (1), the initial iteration value of vibration response $\mathbf{q}^{(0)}$ obtained in the step (2) and the nonlinear stiffness matrix obtained in the step (4) into Eq. (36) to calculate the residual vector \mathbf{r} . Then, employ Eq. (39) to separate the real part and the imaginary part of the residual vector, and substitute the initial value of vibration response $\mathbf{q}^{(0)}$ into

648
649
650
651
652
653
654
655
656
657
658
659
660
661
662
663
664
665
666
667
668
669
670
671
672
673
674
675
676
677
678
679
680
681
682
683
684
685
686
687
688
689
690
691
692
693
694
695
696
697
698
699
700
701
702
703
704
705
706

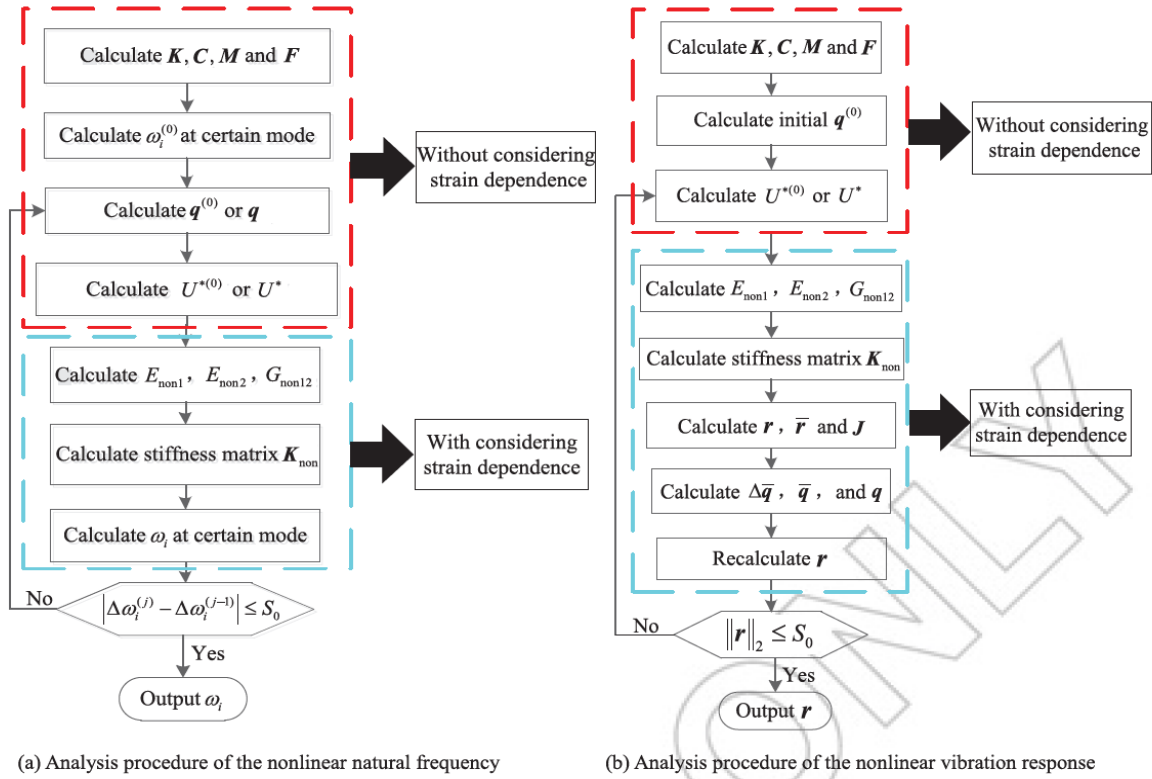


Figure 2. Flowchart of the nonlinear analysis of natural frequencies and vibration responses of the fiber-reinforced composite plate.

Eq. (37) to Eq. (38) to calculate $\partial \mathbf{r} / \partial \mathbf{q}_R$ and $\partial \mathbf{r} / \partial \mathbf{q}_I$. Finally, by bringing these results into Eq. (36), Jacobian matrix \mathbf{J} can be obtained.

7. Iteratively calculate the nonlinear vibration response of the composite plate.

This step includes three sub-steps. Firstly, by substituting the initial iteration value of the vibration response $\mathbf{q}^{(0)}$ and the separated residual vector $\bar{\mathbf{r}}$ and Jacobian matrix \mathbf{J} into Eq. (41), the response vector $\mathbf{q}^{(j)}$ under the chosen excitation frequency ω can be obtained by considering the strain-dependent nonlinearity. Then, recalculate the residual vector $\mathbf{r}^{(j)}$ and consider the iteration termination condition in Eq. (42). If the resulting $\mathbf{r}^{(j)}$ do not meet the requirement of S_0 , the response vector $\mathbf{q}^{(j)}$ is used to recalculate response vector $\mathbf{q}^{(j+1)}$ and residual vector $\mathbf{r}^{(j+1)}$ until the iteration termination condition is satisfied. Finally, by substituting the final response vector \mathbf{q} into Eq. (19), the nonlinear vibration response under the chosen excitation frequency ω can be obtained. By repeating the step (2) to step (7), the nonlinear vibration response of every frequency point in the concerned frequency range can also be acquired. In order to make it clear, the flowchart of the nonlinear analysis of natural frequencies and vibration responses are plotted, as seen in Figures 2a and b.

4. A case study

In this section, a TC300 carbon/epoxy composite plate is taken as a research object, and its nonlinear natural

frequencies and vibration responses under different excitation levels are obtained in the experiment. By comparing the resulting frequency and response results, the practicability and reliability of the theoretical model based on the strain energy density function method can be verified.

4.1 The stress-strain measurement

The studied TC300 carbon/epoxy composite plate is symmetrically laid, which has totally 21 layers with the laminate configuration of $[(0/90)_5/0/(90/0)_5]$ and volume fraction of 45%. Each layer has the same thickness and fiber volume fraction with the longitudinal elastic modulus of 110.0 GPa, transverse elastic modulus of 9.5 GPa, shear modulus of 4.6 GPa, Poisson's ratio of 0.33, and density of 1780 kg/m³. According to the literature [29], its stress-strain curves can be obtained empirically by the corresponding beam specimens with the same fiber material and layer parameters, i.e., the longitudinal and transverse curve can be obtained by the tension test on 0 and 90° composite beams, while the shear stress-strain curve can be determined from by the unidirectional test on a $\pm 45^\circ$ composite beam, which is based on the assumption that the stress-strain response of a single lamina of the unidirectional composite is the same as the response of the total test on the composite structure.

In this research, the universal testing machine (WDW-100E) made by Jinan TimeShijin Instruments Co. Ltd., Jinan, China is employed to measure the stress-strain relations in different fiber directions. According to the test, standard and procedures proposed in the ASTM D3039M-00,

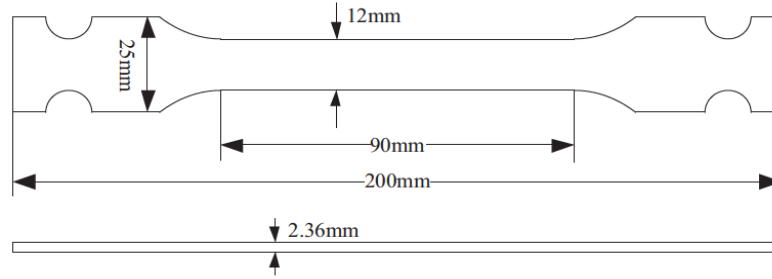


Figure 3. Dimension of tension specimen.

the composite beam is cut off from a large composite plate. Each test specimen and the dimension parameters are illustrated in Figure 3. Besides, the electronic extensometer is attached longitudinally to the center of the specimens to determine the actual value of the tensile displacement. In order to avoid the damage and crushing of the composite beams caused by the clamping tools, the two aided fixtures are also designed, as seen in Figure 4, which are used to well hold each beam specimen. Then, they are installed in the two clamping tools of the machine.

After finishing the clamping and installation process of the composite beam specimens, the tension measurements are carried out with the stretching speed of 0.5 mm/min. Figure 4 gives the real static test picture of the composite beam specimen, and the load-displacement diagrams can be plotted by the corresponding software. Finally, the stress-strain curves in different fiber directions (0° , 90° , and $\pm 45^\circ$) can be obtained indirectly in the software. Figure 5 gives the measured stress-strain curves in the longitudinal, transverse and shear directions. Table 1 lists the initial curvature A_i and the variation B_i in the strain energy destiny function of $E_{\text{non}1}(U^*)$, $E_{\text{non}2}(U^*)$ and $G_{\text{non}12}(U^*)$.

4.2 Nonlinear vibration measurement

In order to accurately measure the nonlinear natural frequencies and vibration responses of the composite plate, the following vibration test system is set up, and its schematic and real test picture can be seen in Figures 6 and 7. The clamp fixture and M8 bolts, as seen in Figure 6, are used to clamp one side of the composite plate to simulate the cantilever constraint boundary condition, and its length, width, and thickness after being clamped is about 200, 130, and 2.36 mm, respectively. The laser point is about 30 mm above the constraint end and the horizontal distance between this point to the left free edge of the plate is about 86 mm. In practice, in order to ensure the tested plate is effectively clamped, the first three natural frequencies are measured under different tightening torques. Through comparison of each other, the best repeatability of frequency values can be reached when the tightening torque is 50 Nm, so this torque value is used in the formal test.

The instruments used in the test are as follow: (I) king-design EM-1000F vibration shaker systems; (II) Polytec PDV-100 laser Doppler vibrometer; (III) BK 4514-001 accelerometer; (VI) LMS SCADAS 16-channel Mobile Front-End

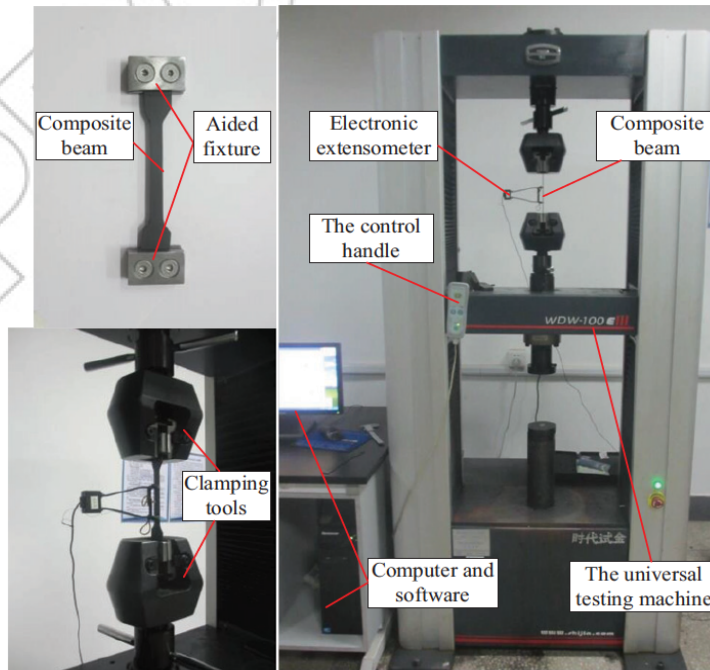


Figure 4. The real test picture of static tension test of the fiber-reinforced composite thin plate. (a) Longitudinal, (b) Transverse, and (c) Shear.

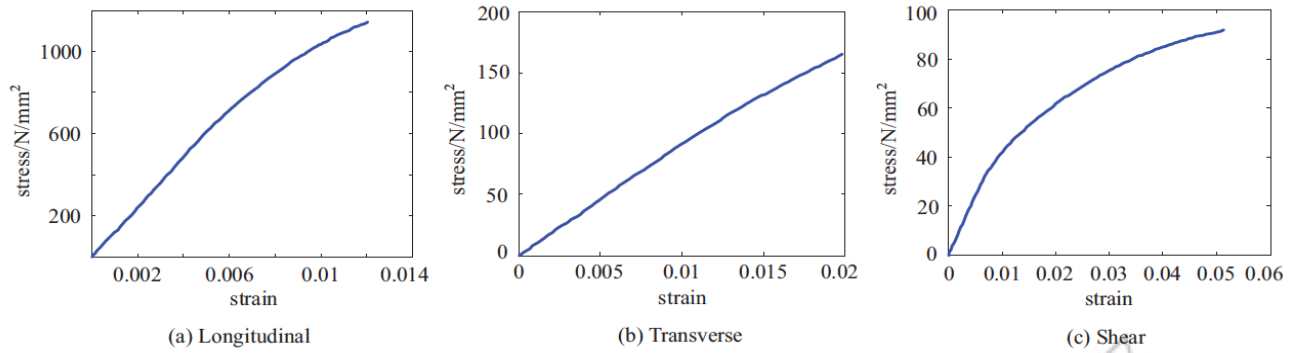


Figure 5. The measured stress-strain curves of the composite beam in different fiber directions.

Table 1. The initial curvature and the variation values of the stress-strain curves of the composite beam.

| Material | A_1 | A_2 | A_{12} | B_1 | B_2 | B_{12} |
|--------------------|-------------------------|--------|----------|--------|--------|----------|
| TC300 carbon/epoxy | 3.4824×10^{-4} | 0.0763 | 1.7768 | 0.0022 | 3.3363 | 36.3159 |

and Dell notebook computer. In the test set-up, the vibration shaker is used to provide base excitation without bringing additional mass and stiffness to the tested structure, the laser Doppler vibrometer, placed to a rigid support, is used to measure the velocity of the plate at a single point along the excitation direction of vibration shaker, while the base response signal is simultaneously acquired by the accelerometer. Besides, LMS SCADAS 16-channel data acquisition front-end is responsible for recording these signals and Dell notebook computer (with Intel Core i7 2.93 GHz processor and 4G RAM) is used to operate LMS Test. Lab 10B software and store signal data. Because the vibration velocity signals are usually obtained by laser Doppler vibrometer, Simpson integral operation should be used in the Test. Lab 10B software to get the displacement signals.

On the one hand, in order to analyze the nonlinear vibration characteristic of the fiber-reinforced composite plate, it is necessary to measure each natural frequency and damping ratio to provide input parameters for the iteration calculation. First, the sine sweep test is done on the plate by selecting sweeping frequency range of 0~1024 Hz with the frequency resolution of 0.2 Hz, base excitation amplitude of 1 g and quick sweep speed of 5 Hz/s, and consequently, the raw sweep signal can be recorded. Next, employ FFT processing technique and hanning window operation to get the frequency spectrum of the signal, and the first six natural frequencies can be roughly determined by identifying the response peak in the spectrum. At last, reselect sweeping frequency range which contains imprecise value of natural frequency and set much slower sweeping speed such as 1 Hz/s to obtain the related frequency spectrum, and each natural frequency and damping ratio can be accurately determined by half-power bandwidth technique, as listed in Table 2.

On the other hand, the nonlinear vibration test on the composite plate is done under different base excitation levels, and each sweeping frequency range should contain each natural frequency result listed in Table 2. By taking the third and the sixth nonlinear natural frequency and vibration response as an example, firstly set the excitation as total five

excitation levels, namely, 1, 2, 3, 4, and 5 g, and then choose much slower sweeping speed such as 1 Hz/s to accurately obtain the corresponding frequency response spectrums containing the third and the sixth natural frequency under each excitation level, as seen in Figures 8 and 9.

4.3 The comparison between the theoretical calculation and experiment

When the experimental test work has been done, according to the analysis procedure of the nonlinear natural frequency proposed in Section 3.1, the linear natural frequency of the composite plate without considering the strain-dependent nonlinearity is calculated firstly. Table 3 lists the first six natural frequency results under the 1 g excitation level which are calculated without considering the strain-dependent nonlinearity, and the theoretical results are also compared with the experimental results.

By considering the strain-dependent nonlinear characteristic, the nonlinear natural frequencies and vibration responses are solved. First, the initial iteration values of the natural frequency, vibration response, and strain energy density of the composite plate are calculated, to obtain the nonlinear material parameters and nonlinear stiffness matrix. Meanwhile, the measured modal damping ratios (which is listed in Table 2) is substituted into Eq. (32) to solve damping matrix, so that the vibration equation in the frequency domain can be acquired.

Still the third and the sixth modes of composite plate are taken for an example. With the same base excitation levels employed in the experiment, the iterative calculation work of the nonlinear natural frequency and vibration response is finished. The third and sixth frequency response spectrums with considering the strain-dependent nonlinearity under different excitation levels are given in Figures 10 and 12. In order to compare the corresponding results conveniently, the related frequency response spectrums without considering the strain-dependence are also obtained, as seen in Figures 11 and 13. Finally, through identifying the above frequency response spectrums, the third and sixth natural frequency and resonant response results with and without considering the strain-dependence are obtained and listed in the Tables 4 and 5. Their calculation errors compared with the experimental results are also listed in the same tables.

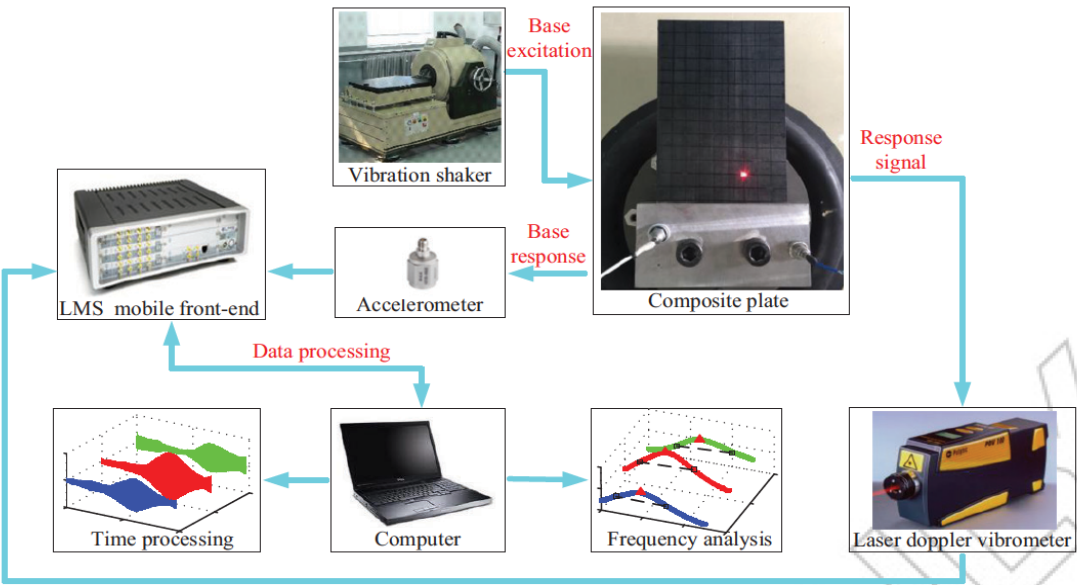


Figure 6. Schematic of the vibration test system of the fiber-reinforced composite thin plate.

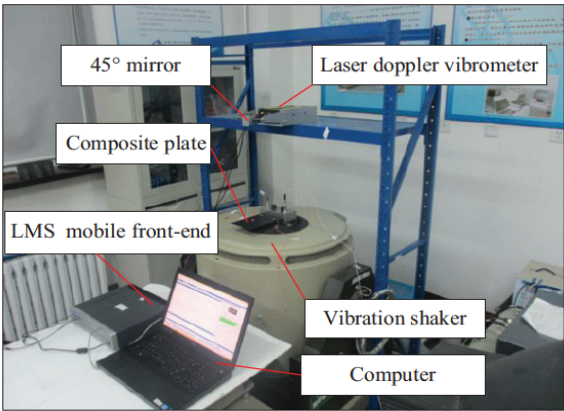


Figure 7. The real test picture of the vibration test system of the fiber-reinforced composite thin plate.

Table 2. The first six natural frequencies and damping ratios of the studied fiber-reinforced composite plate obtained by experimental test.

| Modal order | 1 | 2 | 3 | 4 | 5 | 6 |
|------------------------|------|------|-------|-------|-------|-------|
| Natural frequency (Hz) | 47.6 | 98.4 | 296.5 | 381.6 | 715.6 | 863.8 |
| Damping ratio (%) | 0.47 | 0.50 | 0.57 | 0.92 | 1.05 | 0.94 |

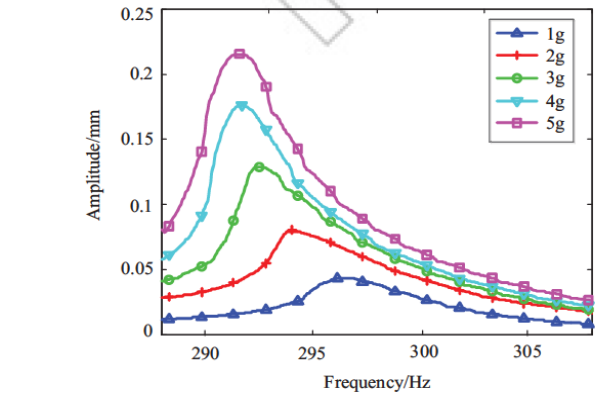


Figure 8. The measured frequency response spectra containing the 3rd natural frequency under different excitation levels.

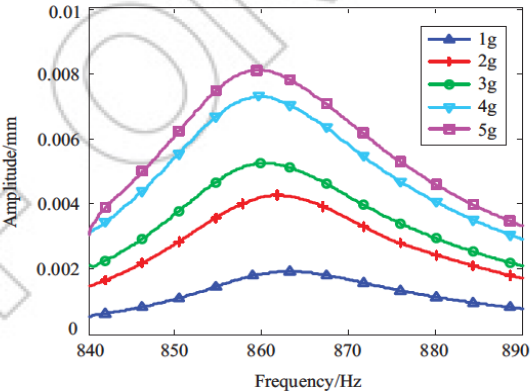


Figure 9. The measured frequency response spectra containing the 6th natural frequency under different excitation levels.

Table 3. The first six natural frequency results calculated without considering the strain-dependent nonlinearity and their errors compared with the experimental results.

| Modal order | 1 | 2 | 3 | 4 | 5 | 6 |
|---------------------------|------|-------|-------|-------|-------|-------|
| Experimental test A (Hz) | 47.6 | 98.4 | 296.5 | 381.6 | 715.6 | 863.8 |
| Theory calculation B (Hz) | 49.2 | 103.5 | 308.2 | 402.3 | 743.2 | 882.6 |
| Errors (%) $ B - A /A$ | 3.4 | 5.2 | 4.4 | 5.4 | 3.9 | 2.2 |

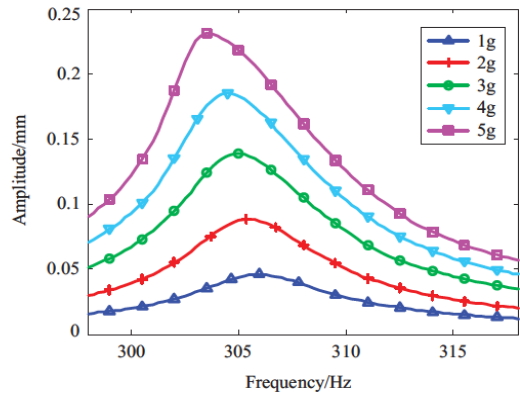


Figure 10. The calculated third frequency response spectra with considering the strain-dependent nonlinearity.

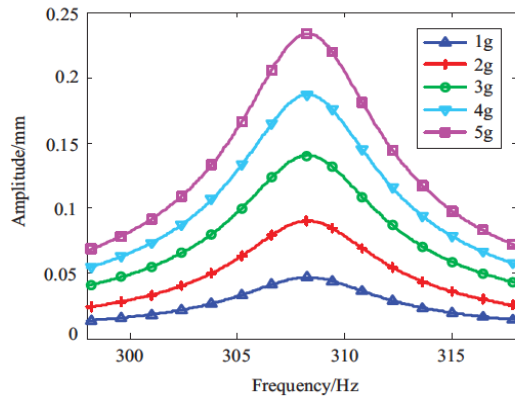


Figure 11. The calculated third frequency response spectrums without considering the strain-dependent nonlinearity.

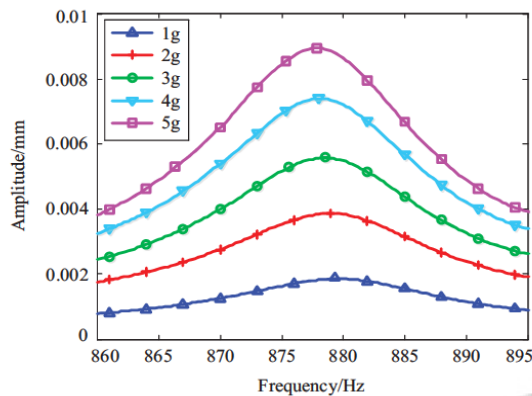


Figure 12. The calculated sixth frequency response spectrums with considering the strain-dependent nonlinearity

As can be seen from Table 3, the first six natural frequencies of the composite plate without considering the strain-dependent nonlinearity show a good agreement with the experimental results, since the theoretical calculation errors are within the range of 2.2%~5.4%. Therefore, this nonlinear calculation method can be used to analyze the natural frequency of the composite plate when we do not care about the strain-dependent nonlinear characteristic.

As also can be seen from Figures 10 to 13, Tables 4 and 5, the third and sixth natural frequency results calculated under different excitation levels can comply well with the same rule discovered in experimental test. i.e., the natural frequencies of the composite plate will decrease with the increase of the base excitation level, which show the soft

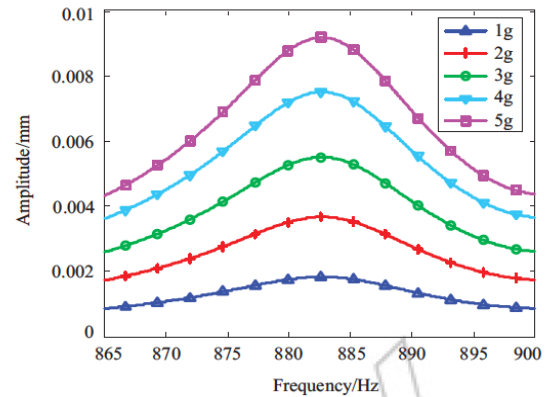


Figure 13. The calculated sixth frequency response spectrums without considering the strain-dependent nonlinearity.

stiffness nonlinearity or “strain softening”. Besides, we can also found out that the frequency errors with considering the strain-dependent nonlinearity (the maximum error is 4.3 and 2.1% in the third and sixth natural frequencies) are smaller than the corresponding errors without considering strain-dependence (the maximum error is 5.9 and 2.7% in the third and sixth natural frequencies).

Then, the linear and nonlinear vibration responses of the composite plate are our focus. The response errors for the third mode and the sixth mode are about 2.7%~14.0%, which are within an acceptable range. Therefore, the practicability and reliability of the strain energy density function method have been verified, which can be used to calculate nonlinear vibration response of the fiber-reinforced composite plate. Besides, the maximum response errors in the third mode and the sixth mode without considering the strain-dependent nonlinearity are 12.6 and 14.0%, while the response errors in the corresponding modes obtained with considering the strain-dependence are less than 12.0%, so by taking the strain-dependent characteristic into account, the more accurate resonant response results can be acquired by strain energy density function method.

However, the maximum error of the calculated resonant responses can still reach to 14.0%. Also, the response errors in the third and sixth frequency response spectrums between the experiment and theoretical calculation still exist, which might be due to the following reasons: (I) the laser point in the experimental test and response point chosen in the theoretical model are not closely coincident, and the cantilever constraint boundary used in the experiment cannot totally

Table 4. The calculated third natural frequencies and resonant responses of the composite plate under different excitation levels with and without considering the strain-dependent nonlinearity and their errors compared with the experimental results.

| Excitation Level (g) | Experimental results | | Theoretical results without considering the nonlinearity | | | | Theoretical results with considering the strain-dependent nonlinearity | | | |
|----------------------|-------------------------|-------------------------|--|-------------------------|----------------------------------|---------------------------------|--|-------------------------|----------------------------------|---------------------------------|
| | Natural Frequency A(Hz) | Resonant response B(mm) | Natural Frequency C(Hz) | Resonant response D(mm) | Frequency errors $ C - A /A$ (%) | Response errors $ D - B /B$ (%) | Natural frequency E(Hz) | Resonant response F(mm) | Frequency errors $ E - A /A$ (%) | Response errors $ F - B /B$ (%) |
| 1 | 296.5 | 0.0439 | 308.3 | 0.0467 | 4.0 | 6.4 | 305.9 | 0.0461 | 3.2 | 5.0 |
| 2 | 295.3 | 0.0785 | 308.3 | 0.0884 | 4.4 | 12.6 | 305.5 | 0.0879 | 3.5 | 12.0 |
| 3 | 293.7 | 0.1286 | 308.3 | 0.1401 | 5.0 | 8.9 | 304.9 | 0.1386 | 3.8 | 7.8 |
| 4 | 292.2 | 0.1760 | 308.3 | 0.1868 | 5.5 | 6.1 | 304.4 | 0.1849 | 4.2 | 5.1 |
| 5 | 291.0 | 0.2154 | 308.3 | 0.2335 | 5.9 | 8.4 | 303.6 | 0.2311 | 4.3 | 7.3 |

Table 5. The calculated sixth natural frequencies and resonant responses of the composite plate under different excitation levels with and without considering the strain-dependent nonlinearity and their errors compared with the experimental results.

| Excitation Level (g) | Experimental results | | Theoretical results without the considering nonlinearity | | | | Theoretical results with considering the strain-dependent nonlinearity | | | |
|----------------------|-------------------------|-------------------------|--|-------------------------|----------------------------------|---------------------------------|--|-------------------------|----------------------------------|---------------------------------|
| | Natural frequency A(Hz) | Resonant response B(mm) | Natural frequency C(Hz) | Resonant response D(mm) | Frequency errors $ C - A /A$ (%) | Response errors $ D - B /B$ (%) | Natural frequency E(Hz) | Resonant response F(mm) | Frequency errors $ E - A /A$ (%) | Response errors $ F - B /B$ (%) |
| 1 | 863.8 | 0.0019 | 882.6 | 0.0018 | 2.2 | 5.3 | 879.6 | 0.0018 | 1.8 | 5.3 |
| 2 | 861.7 | 0.0043 | 882.6 | 0.0037 | 2.4 | 14.0 | 879 | 0.0039 | 2.0 | 9.3 |
| 3 | 860.4 | 0.0052 | 882.6 | 0.0055 | 2.6 | 5.8 | 878.4 | 0.0054 | 2.1 | 3.8 |
| 4 | 859.8 | 0.0073 | 882.6 | 0.0077 | 2.7 | 5.5 | 878.1 | 0.0075 | 2.1 | 2.7 |
| 5 | 859.5 | 0.0081 | 882.6 | 0.0092 | 2.7 | 13.6 | 877.8 | 0.0088 | 2.1 | 8.6 |

equivalent to the ideal boundary condition for the theoretical calculation; (II) in the theoretical modeling process, the following effects are not considered, such as the transverse shear stress, irregular fiber arrangement, interface defect and residual stress; and (III) compared with the real values, there are some errors in the material parameters used in the theoretical calculation due to the dispersivity of the fiber-reinforced composite.

5. Conclusions

This research proposes the strain energy density function method to analyze the nonlinear vibration of the fiber-reinforced composite thin plate with strain-dependent property, and the experimental test is used to verify the practicability and reliability of this nonlinear calculation method.

1. By introducing Jones-Nelson material nonlinearity into the vibration field, the elastic modulus of the fiber composite can be expressed as a function of the strain energy density, and the nonlinear vibration solution of the composite plate can be solved by using the iterative calculation techniques.
2. Based on the theoretical model, the specific analysis procedure of the nonlinear natural frequencies and vibration responses of the composite plate are summarized and proposed.
3. Strain energy density function method is an effective theoretical analysis method to calculate the nonlinear natural frequency and vibration response of the composite plate, and the calculated results comply with the same rule discovered in the experimental test. Both indicate that the natural frequency of the composite plate decrease with the increase of external excitation level, which shows the soft stiffness nonlinearity or “strain softening”.

Disclosure statement

No potential conflict of interest was reported by the authors.

Funding

This study was supported by the National Natural Science Foundation of China granted No. 51505070, the Fundamental Research Funds for the Central Universities of China granted No. N150304011, N160313002 and N160312001, the Scholarship Fund of China

Scholarship Council (CSC) granted No. 201806085032, and the Key Laboratory of Vibration and Control of Aero-Propulsion System Ministry of Education, Northeastern University, granted No.VCAME201603.

ORCID

Hui Li  <http://orcid.org/0000-0002-8639-1203>

References

[1] P. Morgan, Carbon Fibers and Their Composites[M]. Boca Raton, FL: The Chemical Rubber Company Press, 2005.

[2] P. K. Mallick, Fiber-reinforced Composites: Materials, Manufacturing, and Design[M]. Boca Raton, FL: The Chemical Rubber Company Press, 2007.

[3] C. Leyens, F. Kocian, J. Hausmann, and W. A. Kayssera, “Materials and design concepts for high performance compressor components[J],” *Aerosp. Sci. Technol.*, vol. 7, no. 3, pp. 201–210, 2003.

[4] J. R. Vinson, R. L. Sierakowski, and C. W. Bert, The Behavior of Structures Composed of Composite Materials[M]. Netherlands: Springer, 2008.

[5] T. B. Stecenko and M. Stevanovi, “Variation of elastic moduli with strain in carbon/epoxy laminates[J],” *J. Compos. Mater.*, vol. 24, no. 11, pp. 1152–1158, 1990.

[6] B. N. Rao and S. R. Pillai, “Non-linear vibrations of a simply supported rectangular antisymmetric cross-ply plate with immovable edges[J],” *J. Sound Vib.*, vol. 152, no. 3, pp. 568–572, 1992.

[7] G. Singh, G. V. Rao, and N. G. R. Iyengar, “Non-linear forced vibrations of antisymmetric rectangular cross-ply plates[J],” *Compos. Struc.*, vol. 20, no. 3, pp. 185–194, 1992.

[8] P. Ribeiro and M. Petyt, “Non-linear vibration of composite laminated plates by the hierarchical finite element method[J],” *Compos. Struct.*, vol. 46, no. 3, pp. 197–208, 1999.

[9] J. Chen, D. J. Dawe, and S. Wang, “Nonlinear transient analysis of rectangular composite laminated plates[J],” *Compos. Struc.*, vol. 49, no. 2, pp. 129–139, 2000.

[10] Y. Y. Lee and C. F. Ng, “Nonlinear response of composite plates using the finite element modal reduction method[J],” *Eng. Struc.*, vol. 23, no. 9, pp. 1104–1114, 2001.

[11] B. Harras, R. Benamar, and R. G. White, “Geometrically non-linear free vibration of fully clamped symmetrically laminated rectangular composite plates[J],” *J. Sound Vib.*, vol. 251, no. 4, pp. 579–619, 2002.

[12] N. Toyama and J. Takatsubo, “An investigation of non-linear elastic behavior of CFRP laminates and strain measurement using Lamb waves[J],” *Compos. Sci. Technol.*, vol. 64, no. 16, pp. 2509–2516, 2004.

[13] A. K. Onkar and D. Yadav, “Forced nonlinear vibration of laminated composite plates with random material properties[J],” *Compos. Struc.*, vol. 70, no. 3, pp. 334–342, 2005.

- [14] A. Tabiei, W. Yi, and R. Goldberg, "Non-linear strain rate dependent micro-mechanical composite material model for finite element impact and crashworthiness simulation[J]," *Int. J. Non-Lin. Mech.*, vol. 40, no. 7, pp. 957–970, 2005.
- [15] L. Zhu, A. Chattopadhyay, and R. K. Goldberg, "Nonlinear transient response of strain rate dependent composite laminated plates using multiscale simulation[J]," *Int. J. Solids Struct.*, vol. 43, no. 9, pp. 2602–2630, 2006.
- [16] M. K. Singha and R. Daripa, "Nonlinear vibration of symmetrically laminated composite skew plates by finite element method[J]," *Int. J. Non-Lin. Mech.*, vol. 42, no. 9, pp. 1144–1152, 2007.
- [17] Z. Kazancı and Z. Mecitoğlu, "Nonlinear dynamic behavior of simply supported laminated composite plates subjected to blast load[J]," *J. Sound Vib.*, vol. 317, no. 3–5, pp. 883–897, 2008.
- [18] M. K. Singha and R. Daripa, "Nonlinear vibration and dynamic stability analysis of composite plates[J]," *J. Sound Vib.*, vol. 328, no. 4, pp. 541–554, 2009.
- [19] A. G. Arani, S. Maghamikia, and M. Mohammadimehr, A. Arefmanesh, "Buckling analysis of laminated composite rectangular plates reinforced by SWCNTs using analytical and finite element methods[J]," *J. Mech. Sci. Technol.*, vol. 25, no. 3, pp. 809–820, 2011.
- [20] A. G. Arani and G. S. Jafari, "Nonlinear vibration analysis of laminated composite Mindlin micro/nano-plates resting on orthotropic Pasternak medium using DQM[J]," *Appl. Mathe. Mech.*, vol. 36, no. 8, pp. 1033–1044, 2015.
- [21] A. G. Arani, E. Haghparsat, and H. B. A. Zarei, "Vibration of axially moving 3-phase CNTFPC plate resting on orthotropic foundation[J]," *Struc. Eng. Mech.*, vol. 57, no. 1, pp. 105–126, 2016.
- [22] A. R. Setoodeh and M. Shojaee, "Application of TW-DQ method to nonlinear free vibration analysis of FG carbon nanotube-reinforced composite quadrilateral plates[J]," *Thin-Walled Struct.*, vol. 108, pp. 1–11, 2016.
- [23] G. Jiang, F. Li, and X. Li, "Nonlinear vibration analysis of composite laminated trapezoidal plates[J]," *Steel Compos. Struct.*, vol. 21, no. 2, pp. 395–409, 2016.
- [24] Y.Y. Chai, F.M. Li, and Z.G. Song, "Nonlinear vibration behaviors of composite laminated plates with time-dependent base excitation and boundary conditions[J]," *Int. J. Nonlin. Sci. Numer. Simul.*, vol. 18, no. 2, pp. 145–161, 2017.
- [25] R. M. Jones and D. A. R. Nelson, "A new material model for the nonlinear biaxial behavior of ATJ-S graphite[J]," *J. Compos. Mater.*, vol. 9, no. 1, pp. 10–27, 1975.
- [26] R. M. Jones and H. S. Morgan, "Analysis of non-linear stress-strain behavior of fiber-reinforced composite materials[J]," *AIAA J.*, vol. 15, pp. 1669–1676, 1977.
- [27] M. W. Hyer and S. R. White, *Stress Analysis of Fiber-reinforced Composite Materials [M] Stress Analysis of Fiber-reinforced Composite Materials*, New York: WCB McGraw-Hill, pp. 123–128, 1998.
- [28] J. M. Whitney and J. E. Ashton, "Effect of environment on the elastic response of layered composite plates[J]," *AIAA J.*, vol. 9, no. 9, pp. 1708–1713, 1971.
- [29] P. H. Petit and M. E. Waddoups, "A method of predicting the nonlinear behavior of laminated composites[J]," *J. Compos. Mater.*, vol. 3, no. 1, pp. 2–19, 1969.